Article

A Biomechanical Study of Various Fixation Strategies for the Treatment of Clavicle Fractures Using Three-Dimensional Upper-Body Musculoskeletal Finite Element Models

Kao-Shang Shih [1,2], Ching-Chi Hsu [3,*] and Bo-Yu Shih [3]

[1] Department of Orthopedic Surgery, Shin Kong Wu Ho-Su Memorial Hospital, Taipei 111, Taiwan; scorelin@gmail.com
[2] School of Medicine, College of Medicine, Fu Jen Catholic University, New Taipei City 242, Taiwan
[3] Graduate Institute of Applied Science and Technology, National Taiwan University of Science and Technology, Taipei 106, Taiwan; shotb1@gmail.com
* Correspondence: hsucc@mail.ntust.edu.tw

check for updates

Abstract: Plate or nail fixations have been applied to the repair of clavicle fractures. However, it is quite difficult to fairly evaluate the different clavicle fixation techniques owing to variations in the bone anatomy, bone quality, and fracture pattern. The purpose of this study was to investigate the biomechanical performances of different fixation techniques applied to a clavicle fracture using the finite element method. A simplified single-clavicle model and a complete human upper-body skeleton model were developed in this study. Three types of plate fixations, namely, superior clavicle plate, anterior clavicle plate, and clavicle anatomic spiral fixations, and one nail fixation, a titanium elastic nail fixation, were investigated and compared. The plate fixation techniques have a better fixation stability compared to the nail fixation technique. However, the nail fixation technique shows lower bone stress and can reduce the risk of a peri-implant fracture compared to the plate fixation techniques. Increasing the number of locking screws for the clavicle plate system can reduce the implant stress. Insertion of the bone plate into the anterior site of the clavicle or a multi-plane fixation is recommended to achieve the required biomechanical performance. A plate fixation revealed a relatively better fixation stability, and a nail fixation showed a lower risk of a peri-implant fracture.

Keywords: clavicle fracture; finite element analysis; plate fixation; nail fixation

1. Introduction

Trauma, repetitive strain, and overuse are the cause of the most common types of shoulder joint injuries [1–3]. Clavicle fractures are a break in the collarbone, which is a long bone that serves as a strut between the sternum and the scapula [4,5]. The symptoms of a broken collarbone include swelling, pain, and an inability to move the shoulder. Implant fixation or nonoperative treatment has been applied to clavicle fractures [6,7]. However, the fixation of a clavicle fracture is associated with certain complications, such as a wound infection, nonunion, implant failure, loss of position, and refracture [8–11]. In vitro and in vivo experiments have been used to evaluate the effects of fixation techniques on the clavicle biomechanics [12,13]. Unfortunately, only one or two clavicle fixation techniques have been selected and discussed in previous studies [14,15]. The strengths and limitations of various clavicle fixation techniques have not been fully investigated. Finite element analysis is a useful technique used to evaluate various surgical fixations and to control the variations in the fracture patterns, bone anatomy, bone quality, and fixation location [16–20]. This numerical method has also

been applied in studies on clavicle biomechanics. Favre et al. [21] developed finite element models of the superior and anteroinferior reconstructions and compared them with those of an intact clavicle when loaded during axial compression and cantilever bending. Pendergast et al. [22] conducted a finite element simulation on a fracture fixated clavicle. Torsion verification and bending simulations have been investigated. Huang et al. [23] developed finite element models of a superior clavicle plate (SCP), an anterior clavicle plate (ACP), and a clavicle anatomic spiral (CAS). The cantilever bending, axial compression, inferior bending, and axial torsion were applied. Although the above studies investigated the biomechanical performances of clavicle fractures treated with different fixation techniques, a clavicle bone with simplified loading and boundary conditions was considered in their finite element simulations. Additionally, forces generated by arm motion or activity can not be considered in a single-clavicle bone. In the present study, three-dimensional finite element models of a simplified single-clavicle bone and a human upper-body skeleton system were developed to evaluate the biomechanical performances of intact and treated clavicles. Four types of clavicle fixation devices were evaluated, namely, SCP, ACP, CAS, and a titanium elastic nail (TEN). The aim of this study was to evaluate the biomechanical outcomes of various clavicle fixation techniques for the treatment of a clavicle fracture using a finite element method.

2. Materials and Methods

2.1. Single-Clavicle Model with Various Fixation Strategies

A simplified single-clavicle model was developed based on computed tomography (CT) scan images and was derived from a commercial model (Zygote Solid Skeleton Model-2nd Generation, Zygote Media Group, American Fork, UT, USA). It was developed from CT scans of a 50th percentile male, and was carefully modeled to retain subtle anatomical nuances unique to specific bones. The original commercial model is solid. Thus, the clavicle model was divided into cortical bone and cancellous bone based on the suggestion of an orthopedic surgeon using a 3D sculpting design software Geomagic Freeform (3D Systems, Rock Hill, SC, USA). Then, the clavicle model was imported into Geomagic Wrap (3D Systems, Rock Hill, SC, USA) to extract surfaces and generate solid model. To prepare an injured model, a middle-third clavicle fracture with a fracture gap of 2 mm was developed using SolidWorks 2019 (SolidWorks Co., Concord, MA, USA).

Four types of clavicle fixation devices were selected to treat the clavicle fracture including the SCP, ACP, CAS, and TEN. The SCP used a six-hole locking compression plate and locking screws, and was implanted into the superior site of the clavicle. The SCP was 94 mm in length, 10 mm in width, and 3 mm in thickness. The ACP also used a six-hole locking compression plate and locking screws, and was implanted into the anterior site of the clavicle. The dimensions of the ACP were the same as those of the SCP. The CAS used a 17-hole locking compression plate and locking screws, and was implanted in the superior site of the distal clavicle and the anterior site of the proximal clavicle according to the clavicle anatomy. The CAS was 135 mm in length, 10 mm in width, and 4.5 mm in thickness. The TEN used a titanium rod with a 4-mm diameter, which was implanted into the clavicular canal from the proximal site to the distal site (Figure 1).

2.2. Human Upper-Body Skeleton Model with Various Surgical Strategies

Based on the same techniques, a complete human upper-body skeleton model was developed in this study. The human upper-body skeleton model consists of the skull, cervical spine (C1–C7), thoracic spine (T1–T5), five pairs of ribs, sternum, costal cartilage, clavicles, scapulae, humeri, radii, and ulnae. Each bone part was modified and reconstructed to develop both cortical bone and cancellous bone, and all bone parts were assembled to develop the human upper-body skeleton model using SolidWorks 2019. A middle-third clavicle fracture with a fracture gap of 2 mm was also considered for the complete upper-body skeleton models.
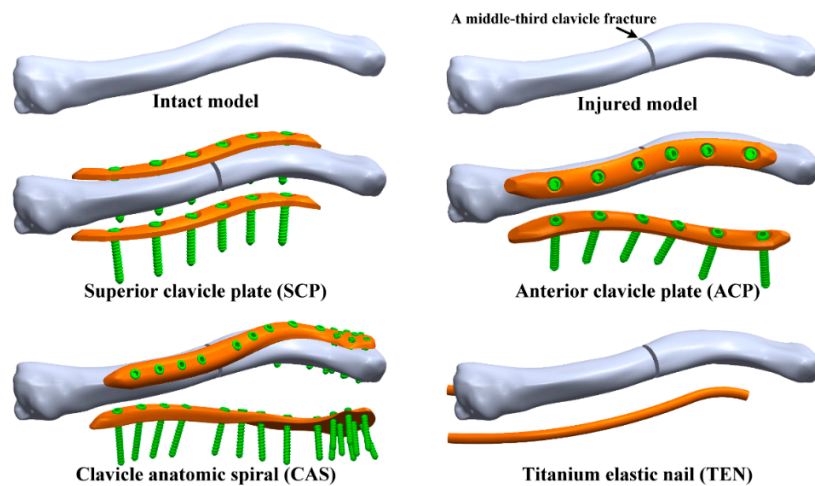
Figure 1. Simplified single-clavicle models.

To prepare the treated models, the SCP, ACP, CAS, and TEN were implanted into the complete upper-body skeleton model. The geometry, dimension, implantation location, and fixation technique of all the clavicle fixation devices used in the complete skeleton model were the same as the single-clavicle model (Figure 2).
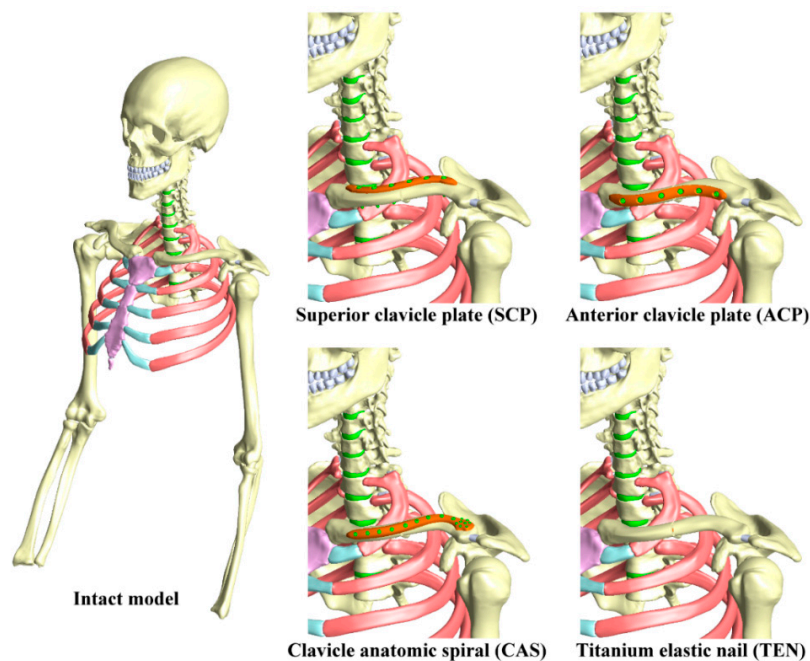

Figure 2. Complete human upper-body models.

2.3. Finite Element Analyses

The finite element models of the intact and treated clavicles were developed using ANSYS Workbench 19.2 (ANSYS, Inc., Canonsburg, PA, USA). The materials used for the fixation devices and bones were assumed to be linearly elastic isotropic. The ligaments and muscles were developed using tension-only spring elements. The stiffness for a muscle was calculated by a formula $K = (E \times A)/L$, where K is the stiffness, E is the Young's modulus, A is the cross-sectional area, and L is the length of a muscle. The insertion points of the ligaments and muscles followed the guidance of an orthopaedic surgeon. All material properties of the finite element models were obtained from previous studies [24–28] and are listed in Table 1. Owing to the complicated and irregular geometries

of the implants and bones, the numerical models were free-meshed using 20-node solid elements of
SOLID 186 (Figure 3). The element size of the finite element models was determined by conducting a
convergent study, and the element size was 0.5 mm for the implants, 2 mm for the clavicle, 8 mm for
the skull, and 4 mm for the others. A frictionless contact interface was defined between the fractured
fragments. For the plate fixations, the following interfaces were assumed to be bonded: the screw head
and the plate, and the screws and the bone. Additionally, a contact interface between the plate and
the bone was considered. For the nail fixation, a contact interface between the nail and the bone was
considered. However, the interface between the proximal clavicle and the proximal nail was assumed
to be bonded. Under the loading and boundary conditions of the single-clavicle model, a bending
force of 200 N [21,29], a compression force of 200 N [21,29], and a combination of the bending and
compression forces were applied to the distal clavicle. Moreover, the proximal clavicle was fully
constrained (Figure 4A). For the human upper-body skeleton model, a load of 200 N was applied to
the distal humerus of the right arm, and the surfaces of the sternum, fifth rib, fifth thoracic vertebra,
and cranium were fully restricted (Figure 4B). During the post-processing, the maximum displacement
of the clavicle, the maximum von Mises stress of the clavicle, and the maximum von Mises stress of the
fixation devices were calculated to investigate each fixation strategy.

Table 1. Material properties of the numerical models.

Materials	Young's Modulus (MPa)	Poisson's Ratio	Area (mm^2)
Skeleton			
Skull	10,000	0.29	-
Teeth	18,600	0.31	-
Clavicle (Cortical bone)	10,000	0.29	-
Clavicle (Cancellous bone)	100	0.29	-
Scapular	16,000	0.3	-
Rib	4520	0.375	-
Sternum	9680	0.3	-
Costal cartilages	24.5	0.4	-
Spine column (Cortical bone)	10,000	0.25	-
Spine column (Cancellous bone)	450	0.25	-
Spine column (Posterior elements)	3500	0.3	-
Spine column (Annulus fibrosus)	4.2	0.45	-
Spine column (Nucleus pulposus)	1	0.499	-
Implants			
Plates/Nail/Screws (Titanium alloy)	114,000	0.3	-
Muscles			
Sternocleidomastoid muscle	0.5	-	246
Trapezius muscle	0.5	-	126
Deltoid muscle	0.5	-	1817
Levator scapulae muscle	0.5	-	126
Supraspinatus muscle	0.5	-	572
Infraspinatus muscle	0.5	-	1374
Pectoralis major muscle	0.5	-	1334
Subscapularis muscle	0.5	-	1630
Ligaments	Stiffness (N/mm)		
Anterior sternoclavicular ligament	50	-	-
Posterior sternoclavicular ligament	50	-	-
Interclavicular ligament	50	-	-
Costoclavicular ligament	50	-	-
Superior acromioclavicular ligament	30	-	-
Inferior acromioclavicular ligament	30	-	-
Coracoclavicular ligament	30	-	-

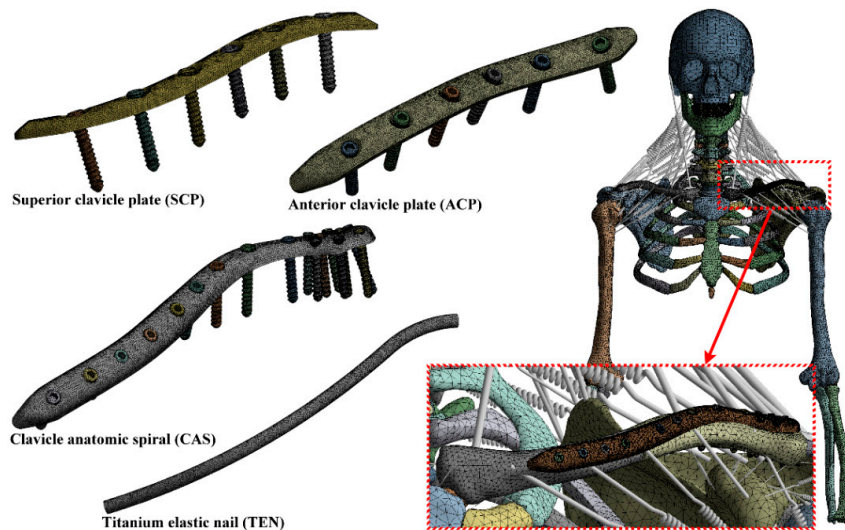| Materials	Young's Modulus (MPa)	Poisson's Ratio	Area (mm^2)
Coracoacromial ligament	30	-	-
Superior transverse scapular ligament	30	-	-
Superior glenohumeral ligament	30	-	-
Middle glenohumeral ligaments	30	-	-
Inferior glenohumeral ligaments	30	-	-
Coracohumeral ligament	30	-	-

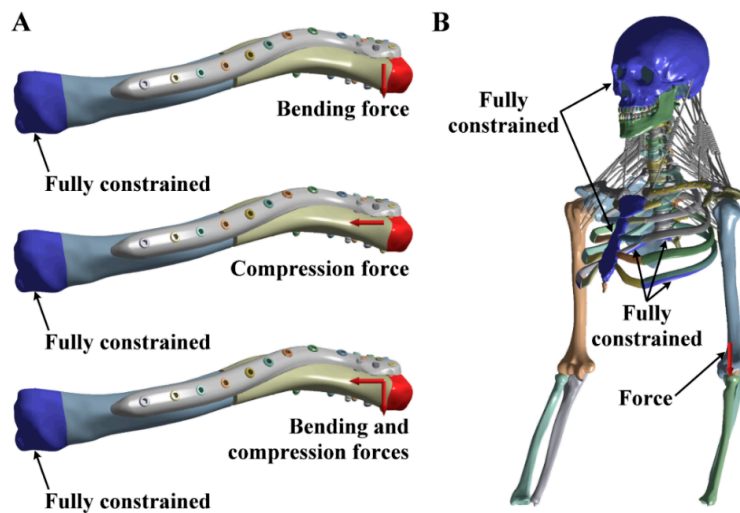**Figure 3.** The meshed finite element models.

Figure 4. Loading and boundary conditions: (**A**) simplified single-clavicle models and (**B**) complete human upper-body models.

2.4. Model Validation and Correlation Analyses

The correlation analyses were conducted to validate the feasibility and applicability of the finite element models developed in the present study. Although no study had compared the intact model, superior plate, anterior plate, spiral plate, and elastic nail, some of the fixation techniques had been investigated by past studies. Thus, the findings obtained by the past studies could be used as the evidences of verification. Favre et al. [21] calculated the normalized compressive rigidity of the intact

model, superior plate, and anterior plate. Their results were compared and correlated with the results of the single-clavicle models during compression loading. Huang et al. [23] calculated the normalized structural stiffness of the superior plate, anterior plate, and spiral plate during two kinds of loadings, namely, bending load and axial compression load. Their results were compared and correlated with the results of the single-clavicle models during bending loading and compression loading, respectively. Zeng et al. [29] calculated the normalized compressive rigidity of the intact model, superior plate, and titanium elastic nail. Their results were also compared and correlated with the results of the single-clavicle models during compression loading. After the validation of the single-clavicle models by the past studies, it was also compared and correlated with the results of the complete upper-body musculoskeletal models to clarify the difference between the simplified models and complete models.

3. Results

3.1. Simplified Single-Clavicle Models

The maximum displacement, clavicle bone stress, and implant stress of all simplified single-clavicle models have properly converged. The numerical error owing to the different element sizes for the maximum displacement of the simplified models was within 3%. In addition, the error due to the different element sizes for both the clavicle bone stress and the implant stress was within 10%. The finite element models of the simplified single-clavicle contained approximately 240,000 to 1,150,000 nodes, and 170,000 to 780,000 elements. The solution time was approximately 0.5 to 2 h. The maximum displacement of the numerical models under the bending load revealed a similar outcome as those under a combined load. The ACP and CAS showed a lower maximum displacement compared to the others under the bending and combined load conditions. This indicates that these two fixation techniques can provide the required fixation stability (Figure 5A). Although the TEN showed the worst fixation stability among all fixation techniques applied, it demonstrated the lowest maximum stress of the clavicle bone. This implies that the TEN has a lower risk of bone fracture after treatment compared to the plate fixation techniques (the SCP, ACP, and CAS) (Figure 5B). In the results of the implant stress, both the ACP and CAS revealed a lower implant stress than the SCP and TEN under bending and combined load conditions (Figure 5C).

3.2. Complete Human Upper-Body Skeleton Models

All numerical outcomes of the complete human upper-body skeleton models properly converged. The numerical error owing to the different element sizes for the maximum displacement of the complete human upper-body models was within 4%. In addition, the error owing to the different element sizes for both the clavicle bone stress and the implant stress was within 10%. The finite element models of the complete human upper-body skeleton contained approximately 1,010,000 to 1,720,000 nodes, and 660,000 to 1,130,000 elements. The solution time was approximately 4 to 7 h. The SCP, ACP, and CAS showed similar maximum displacements or fixation stability, and achieved a better fixation stability than the TEN. This means that the plate fixation techniques can provide the required fixation stability better than that of the nail fixation technique (Figure 6A). The clavicle bone stress of the TEN was significantly lower than that of the SCP, ACP, and CAS. This result indicates that the nail fixation technique has a lower risk of bone fracture after treatment compared to the plate fixation techniques (Figure 6B). The implant stress of both the ACP and CAS is lower than that of the SCP and TEN. The ACP and CAS showed a lower risk of implant failure (Figure 6C). Compared to the results of the simplified single-clavicle models, the numerical outcomes of the complete human upper-body skeleton models were closely related to those of the simplified models under a combined load condition.
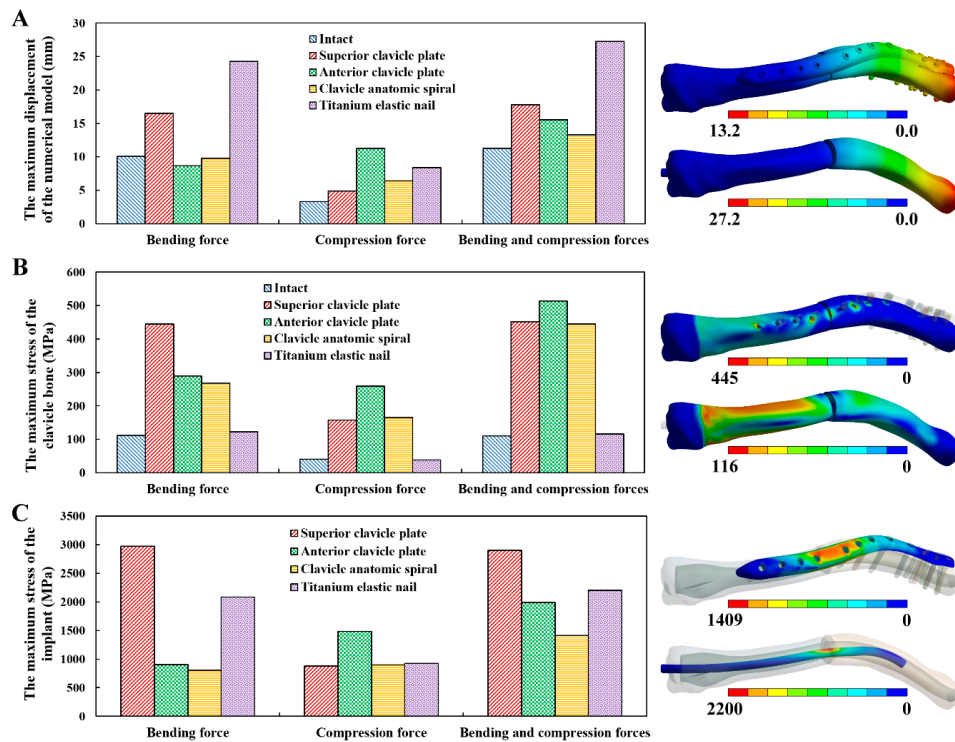
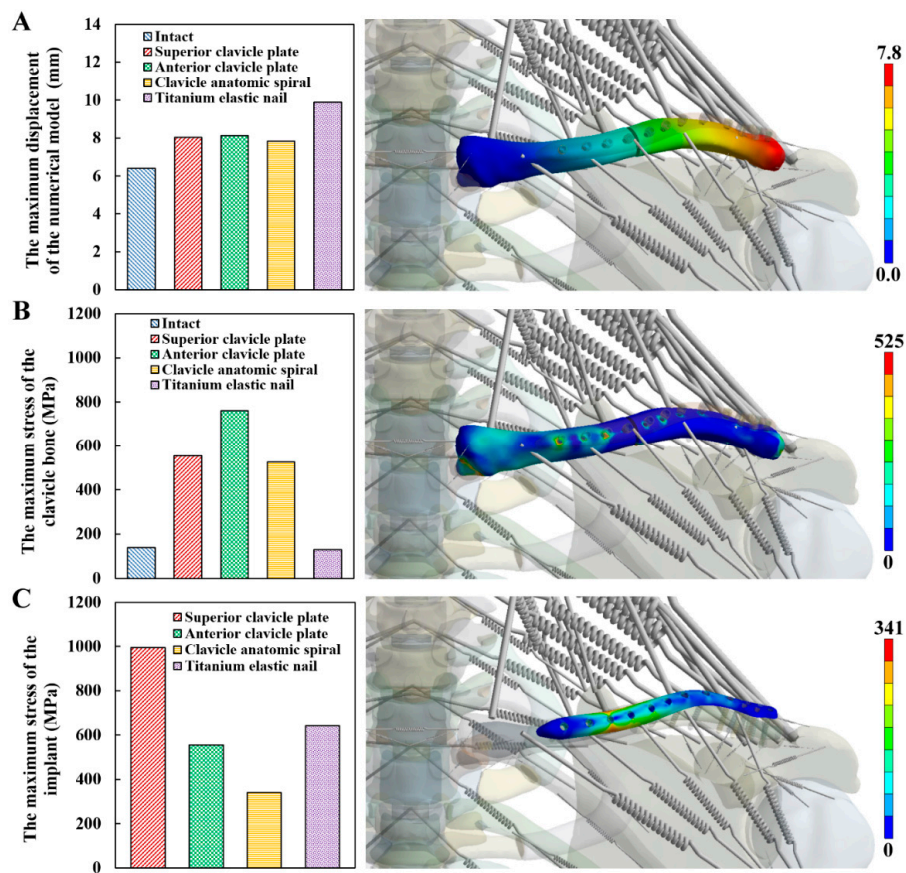**Figure 5.** Results of the simplified models: (**A**) maximum displacement, (**B**) clavicle bone stress, and (**C**) implant stress.

Figure 6. Results of complete human upper-body models: (**A**) maximum displacement, (**B**) clavicle bone stress, and (**C**) implant stress.

3.3. Model Validation and Correlation Analyses

The results of the intact clavicle and broken clavicle after different fixation strategies were validated. The maximum displacement of the intact model, SCP, and ACP during axial compression calculated by the single-clavicle models was correlated with the normalized compressive rigidity obtained by Favre et al. [21]. The result showed that a high correlation coefficient of −0.902 is observed between the present study and Favre et al.'s study (Figure 7A). The results of three different plate fixation strategies were also validated. The maximum displacement of the SCP, ACP, and CAS during bending calculated by the single-clavicle models was correlated to the normalized structural stiffness during bending obtained by Huang et al. [23]. The correlation results indicated that a correlation coefficient of −0.747 is observed (Figure 7B). The similar correlation study for the numerical models during axial compression was conducted, and a high correlation coefficient of −0.912 is observed between the present study and Huang et al.'s study (Figure 7C). Additionally, the results of the plate fixation and nail fixation were verified. The maximum displacement of the intact model, SCP, and TEN during axial compression calculated by the single-clavicle models was correlated to the normalized compressive rigidity obtained by Zeng et al. [29]. The results showed that a correlation coefficient of −0.745 is observed (Figure 7D). The rigidity is the slope of the linear force-displacement curve. Thus, the rigidity was calculated by dividing the applied force by the resulting length change (or displacement). A fixation strategy with a better fixation stability has larger rigidity and smaller displacement. This is a reason why a negative correlation was found in Figure 7A–D.
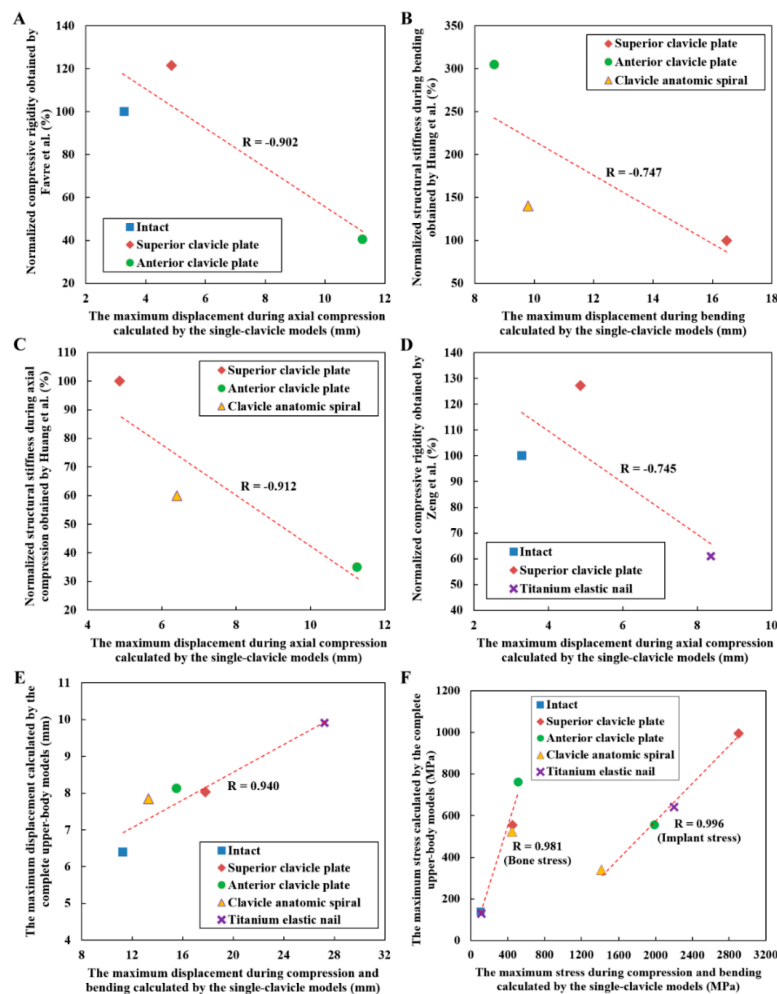

Figure 7. Results of the correlation analyses: (**A**) compared with Favre et al.; (**B**,**C**) compared with Huang et al.; (**D**) compared with Zeng et al.; (**E**,**F**) correlation between the simplified and complete models.

The correlation study between the simplified models and the complete models was conducted. The maximum displacement calculated by the simplified models was closely related to that of the complete models with a high correlation coefficient of 0.940 (Figure 7E). Similarly, the correlation coefficient between the simplified and complete models for the bone stress was found to be 0.981, and 0.996 for the implant stress (Figure 7F).

4. Discussion

Fixation stability is one of the important concerns for bone fracture treatment [30]. In fact, the bone healing time is strongly influenced by the fixation stability [31]. In the present study, the maximum displacement of the clavicle treatments was used to evaluate their fixation stability. The numerical approach showed that the plate fixation techniques demonstrate a better fixation stability than the nail fixation technique. This finding was validated by Zeng et al. [29], who concluded that the TEN provides less stability compared to a reconstruction plate for the treatment of simple displaced fractures of the midshaft clavicle. In addition, van der Meijden et al. [14] also found that the patients in the plate-fixation group recovered faster than the patients in the intramedullary nailing group during the first six months after surgery. Therefore, when considering the fixation stability, the present study suggests the use of a plate fixation for the treatment of a middle-third clavicle fracture. More specifically, both the ACP and CAS can provide the required fixation stability as compared to the SCP and TEN. A fixation strategy with a better fixation stability has smaller displacement, larger rigidity, and higher stiffness. The correlation study (Figure 7A–D) showed that a negative correlation was found between the past studies and the present study. Those results supported the feasibility of the simplified single-clavicle models and the complete human upper-body skeleton models (Figure 7E,F).

A peri-implant fracture is one possible complication of a clavicle treatment [9,32]. Peri-implant stress has been applied to investigate the risk of a peri-implant fracture [16,28,33]. In the present research, the maximum von Mises stress of the clavicle bone was calculated. The results showed that all plate fixations demonstrated a higher clavicle bone stress compared to the nail fixation. This finding is inconsistent with the results by Ni et al. [34], who found that the locking plate fixation shows lower bone stress than that of the Sonoma intramedullary nail and Rockwood clavicle pin. The inconsistency between these studies is due to an assumption of the locking screw geometry. Ni et al. modeled the locking screws as 3.5-mm diameter solid cylinders. However, the present study considered locking screws with a real thread geometry. This means that the threads of the locking screws can cut into the clavicle bone and create a stress riser effect in the bone.

In addition to the fixation stability and a peri-implant fracture, an implant failure is another important issue regarding a clavicle fracture fixation [6,8,35]. In the present study, the maximum von Mises stress of the fixation devices was calculated. The results show that the implant stress of the SCP is higher than that of the ACP in a single-clavicle model under bending and combined loads. This result was verified by Huang et al. [23], who constructed a superior plate, an anterior plate, and a spiral plate with identical cross-sectional features, and found that the implant stress of the superior clavicle plate was higher than that of the anterior clavicle plate. This means that the stress of a clavicle plate is affected significantly by the different fixation positions. However, the stress of a spiral clavicle plate was shown by Huang et al. to be higher than that of an anterior clavicle plate. Their results are inconsistent with the present study, however, in that the CAS has a lower implant stress compared with the ACP, which occurs because Huang et al. constructed all clavicle plates with identical cross-sectional features, whereas the present study did not control for this factor. Although an inconsistency between these two studies was found, an important fact was deduced, namely, increasing the number of locking screws for a spiral clavicle plate can reduce the implant stress and may also decrease the risk of an implant failure.

Plate fixation techniques were demonstrated to have a higher fixation stability than that of a nail fixation technique for the treatment of bone fractures [36,37]. The use of locking screws for the plate fixations can allow the forces of the fractured bones to be shared. However, locking screws need to

cut into bone and create a stress riser effect [38]. The above idea can also be found in the present study. It was shown that plate fixation techniques, which use locking screws to fix the fractured bones, achieve a better fixation stability compared to a nail fixation technique. However, a nail fixation technique, which does not place screw holes in the clavicle, shows lower bone stress and can reduce the risk of a peri-implant fracture compared to plate fixation techniques. Stress in the plate and nail fixations was shown to be affected by various parameters, such as the implant geometry, implant size, and implant material [16,23,28]. In the present study, all plate fixations revealed a different implant stress. Thus, the implant stress of the TEN was higher than that of the CAS and ACP but was lower than that of the SCP. As a reason for this result, the variation in the stress of the clavicle plates occurs from the different plate fixation locations and plate geometries. Thus, to reduce the stress in plate fixation devices, a clavicle plate system inserted into the anterior site of the clavicle bone, or a multi-plane fixation (a spiral plate), was suggested. In addition, increasing the number of locking screws for a clavicle plate system can reduce the implant stress and might also decrease the risk of an implant failure.

The present study has a few limitations that need to be noted. First, the ideal linear elastic material models were applied to the fixation devices and bones during the finite element simulation. Relative comparisons between the different fixation techniques were suggested. Second, all muscles were modeled using tension-only springs and were considered passive elements. These assumptions might not be suitable for modeling the real behavior of the muscles. Third, the cross-sectional features and number of locking screws for the CAS were different compared to those of the SCP and ACP. The comparison between them might have a certain bias. Fourth, a load of 200 N was applied to the distal humerus of the right arm. This loading cannot represent the real loading of the human arm. Fortunately, forces generated by arm motion or activity can be considered in the finite element simulation if the magnitude and orientation of them can be defined. Fifth, a middle-third clavicle fracture with a normal bone quality was considered in this study. The study findings may not apply to all types of clavicle fractures and different bone quality. Fortunately, this methodology can be applied to various specimens to draw the treatment suggestion for general population with clavicle fractures. Finally, both the simplified single-clavicle models and the complete human upper-body skeleton models were derived from a commercial model. Thus, it is a solid model and can not control any CT settings or parameters.

5. Conclusions

The biomechanical performances of different fixation techniques for the treatment of a middle-third clavicle fracture can be investigated using three-dimensional upper-body musculoskeletal finite element simulations. A bone plate inserted into the anterior site of the clavicle, or a multi-plane fixation, is recommended to achieve the required biomechanical performance. Increasing the number of locking screws for the clavicle plate system can reduce the implant stress. A plate fixation revealed a relatively better fixation stability than a nail fixation. However, a nail fixation showed a lower risk of a peri-implant fracture than a plate fixation. Both the simplified single-clavicle models and the complete human upper-body skeleton models can be applied to evaluate different clavicle injuries, fixation strategies, and implant designs in the future. Additionally, arm motion or activity can be considered in the complete human upper-body skeleton model to more realistic evaluate all the performances in the future. Although the findings were validated by previous numerical studies, an experimental validation can be applied to directly verify the feasibility of the upper-body musculoskeletal finite element models.

Author Contributions: Conceptualization, K.-S.S. and C.-C.H.; Formal analysis, C.-C.H. and B.-Y.S.; Funding acquisition, K.-S.S. and C.-C.H.; Investigation, K.-S.S., C.-C.H. and B.-Y.S.; Methodology, C.-C.H.; Validation, K.-S.S., C.-C.H. and B.-Y.S.; Writing—original draft, C.-C.H. and B.-Y.S.; Writing—review & editing, K.-S.S. and C.-C.H. All authors have read and agreed to the published version of the manuscript.

Conflicts of Interest: The authors declare no conflict of interest.

References

1. Sandstrom, C.K.; Kennedy, S.A.; Gross, J.A. Acute shoulder trauma: What the surgeon wants to know. *RadioGraphics* **2015**, *35*, 475–492. [CrossRef] [PubMed]
2. Andersson, S.H.; Bahr, R.; Clarsen, B.; Myklebust, G. Preventing overuse shoulder injuries among throwing athletes: A cluster-randomised controlled trial in 660 elite handball players. *Brit. J. Sport Med.* **2016**, *51*, 1073–1080. [CrossRef] [PubMed]
3. Kannus, P.; Niemi, S.; Sievänen, H.; Parkkari, J. Stabilized incidence in proximal humeral fractures of elderly women: Nationwide statistics from finland in 1970–2015. *J. Gerontol. Ser. A* **2017**, *72*, 1390–1393. [CrossRef]
4. Gilde, A.K.; Hoffmann, M.F.; Sietsema, D.L.; Jones, C.B. Functional outcomes of operative fixation of clavicle fractures in patients with floating shoulder girdle injuries. *J. Orthoped. Traumatol.* **2015**, *16*, 221–227. [CrossRef] [PubMed]
5. Holder, J.; Kolla, S.; Lehto, S. Clavicle fractures: Allman and neer classification. *J. Adv. Radiol. Med. Imag.* **2017**, *2*, 102.
6. Woltz, S.; Stegeman, S.A.; Krijnen, P.; van Dijkman, B.A.; van Thiel, T.P.H.; Schep, N.W.L.; de Rijcke, P.A.R.; Frolke, J.P.M.; Schipper, I.B. Plate fixation compared with nonoperative treatment for displaced midshaft clavicular fractures. *J. Bone Jt. Surg. Am.* **2017**, *99*, 106–112. [CrossRef] [PubMed]
7. Naimark, M.; Dufka, F.L.; Han, R.; Sing, D.C.; Toogood, P.; Ma, C.B.; Feeley, B.T. Plate fixation of midshaft clavicular fractures: Patient-reported outcomes and hardware-related complications. *J. Shoulder Elb. Surg.* **2016**, *25*, 739–746. [CrossRef]
8. Asadollahi, S.; Hau, R.C.; Page, R.S.; Richardson, M.; Edwards, E.R. Complications associated with operative fixation of acute midshaft clavicle fractures. *Injury* **2016**, *47*, 1248. [CrossRef]
9. Santolini, E.; Stella, M.; Sanguineti, F.; Felli, L.; Santolini, F. Treatment of distal clavicle nonunion with and without bone grafting. *Injury* **2018**, *49*, S34–S38. [CrossRef]
10. Frima, H.; Hulsmans, M.H.J.; Houwert, R.M.; Ahmed Ali, U.; Verleisdonk, E.J.M.M.; Sommer, C.; van Heijl, M. End cap versus no end cap in intramedullary nailing for displaced midshaft clavicle fractures: Influence on implant-related irritation. *Eur. J. Trauma Emerg. Surg.* **2017**, *44*, 119–124. [CrossRef]
11. Faust, K.C.; Lark, R.K.; Leversedge, F.J. Pediatric clavicle injuries. In *Clavicle Injuries*; Springer: Cham, Switzerland, 2018; pp. 205–214.
12. Pulos, N.; Yoon, R.S.; Shetye, S.; Hast, M.W.; Liporace, F.; Donegan, D.J. Anteroinferior 2.7-mm versus 3.5-mm plating of the clavicle: A biomechanical study. *Injury* **2016**, *47*, 1642–1646. [CrossRef] [PubMed]
13. Yagnik, G.P.; Brady, P.C.; Zimmerman, J.P.; Jordan, C.J.; Porter, D.A. A biomechanical comparison of new techniques for distal clavicular fracture repair versus locked plating. *J. Shoulder Elb. Surg.* **2019**. [CrossRef] [PubMed]
14. Van der Meijden, O.A.; Houwert, R.M.; Hulsmans, M.; Wijdicks, F.J.G.; Dijkgraaf, M.G.; Meylaerts, S.A.; Hammacher, E.R.; Verhofstad, M.H.J.; Verleisdonk, E.J.M.M. Operative treatment of dislocated midshaft clavicular fractures: Plate or intramedullary nail fixation? *J. Bone Jt. Surg. Am.* **2015**, *97*, 613–619. [CrossRef] [PubMed]
15. Ottomeyer, C.; Taylor, B.C.; Isaacson, M.; Martinez, L.; Ebaugh, P.; French, B.G. Midshaft clavicle fractures with associated ipsilateral acromioclavicular joint dislocations: Incidence and risk factors. *Injury* **2017**, *48*, 469–473. [CrossRef] [PubMed]
16. Lee, C.H.; Hsu, C.C.; Huang, P.Y. Biomechanical study of different fixation techniques for the treatment of sacroiliac joint injuries using finite element analyses and biomechanical tests. *Comput. Biol. Med.* **2017**, *87*, 250–257. [CrossRef] [PubMed]
17. Belli, S.; Eraslan, O.; Eskitaşcıoğlu, G. Effect of different treatment options on biomechanics of immature teeth: A finite element stress analysis study. *J. Endodont.* **2018**, *44*, 475–479. [CrossRef]
18. Mirulla, A.I.; Bragonzoni, L.; Zaffagnini, S.; Bontempi, M.; Nigrelli, V.; Ingrassia, T. Virtual simulation of an osseointegrated trans-humeral prosthesis: A falling scenario. *Injury* **2018**, *49*, 784–791. [CrossRef]
19. Fletcher, J.W.A.; Windolf, M.; Richards, R.G.; Gueorguiev, B.; Varga, P. Screw configuration in proximal humerus plating has a significant impact on fixation failure risk predicted by finite element models. *J. Shoulder Elb. Surg.* **2019**, *28*, 1816–1823. [CrossRef]
20. Ingrassia, T.; Nalbone, L.; Nigrelli, V.; Ricotta, V.; Pisciotta, D. Biomechanical analysis of the humeral tray positioning in reverse shoulder arthroplasty design. *Int. J. Interact. Des. Manuf.* **2017**, *12*, 651–661. [CrossRef]

21. Favre, P.; Kloen, P.; Helfet, D.L.; Werner, C.M.L. Superior versus anteroinferior plating of the clavicle: A finite element study. *J. Orthop. Trauma* **2011**, *25*, 661–665. [CrossRef]

22. Pendergast, M.; Rusovici, R. A finite element parametric study of clavicle fixation plates. *Int. J. Numer. Meth. Biomed. Eng.* **2015**, *31*, e02710. [CrossRef] [PubMed]

23. Huang, T.L.; Chen, W.C.; Lin, K.J.; Tsai, C.L.; Lin, K.P.; Wei, H.W. Conceptual finite element study for comparison among superior, anterior, and spiral clavicle plate fixations for midshaft clavicle fracture. *Med. Eng. Phys.* **2016**, *38*, 1070–1075. [CrossRef]

24. Sarrafpour, B.; Rungsiyakull, C.; Swain, M.; Li, Q.; Zoellner, H. Finite element analysis suggests functional bone strain accounts for continuous post-eruptive emergence of teeth. *Arch. Oral. Biol.* **2012**, *57*, 1070–1078. [CrossRef] [PubMed]

25. Bassett, R.W.; Browne, A.O.; Morrey, B.F.; An, K.N. Glenohumeral muscle force and moment mechanics in a position of shoulder instability. *J. Biomech.* **1990**, *23*, 405–415. [CrossRef]

26. Faizan, A.; Goel, V.K.; Biyani, A.; Garfin, S.R.; Bono, C.M. Adjacent level effects of bi level disc replacement, bi level fusion and disc replacement plus fusion in cervical spine- a finite element based study. *Clin. Biomech.* **2012**, *27*, 226–233. [CrossRef] [PubMed]

27. Ha, S.K. Finite element modeling of multi-level cervical spinal segments (c3–c6) and biomechanical analysis of an elastomer-type prosthetic disc. *Med. Eng. Phys.* **2006**, *28*, 534–541. [CrossRef]

28. Shih, K.S.; Truong, T.A.; Hsu, C.C.; Hou, S.M. Biomechanical investigation of different surgical strategies for the treatment of rib fractures using a three-dimensional human respiratory model. *Biomed. Eng./Biomed. Tech.* **2019**, *64*, 93–102. [CrossRef]

29. Zeng, L.; Wei, H.; Liu, Y.; Zhang, W.; Pan, Y.; Zhang, W.; Zhang, C.; Zeng, B.; Chen, Y. Titanium elastic nail (ten) versus reconstruction plate repair of midshaft clavicular fractures: A finite element study. *PLoS ONE* **2015**, *10*, e0126131. [CrossRef]

30. Ye, Y.; Hao, J.; Mauffrey, C.; Hammerberg, E.M.; Stahel, P.F.; Hak, D.J. Optimizing stability in femoral neck fracture fixation. *Orthopedics* **2015**, *38*, 625–630.

31. Wehner, T.; Claes, L.; Niemeyer, F.; Nolte, D.; Simon, U. Influence of the fixation stability on the healing time—A numerical study of a patient-specific fracture healing process. *Clin. Biomech.* **2010**, *25*, 606–612. [CrossRef]

32. Erdle, B.; Izadpanah, K.; Jaeger, M.; Jensen, P.; Konstantinidis, L.; Zwingmann, J.; Südkamp, N.P.; Maier, D. Comparative analysis of locking plate versus hook plate osteosynthesis of neer type iib lateral clavicle fractures. *Arch. Orthop. Traum Surg.* **2017**, *137*, 651–662. [CrossRef] [PubMed]

33. Lee, C.H.; Shih, C.M.; Huang, K.C.; Chen, K.H.; Hung, L.K.; Su, K.C. Biomechanical analysis of implanted clavicle hook plates with different implant depths and materials in the acromioclavicular joint: A finite element analysis study. *Artif. Organs* **2016**, *40*, 1062–1070. [CrossRef] [PubMed]

34. Ni, M.; Niu, W.; Wong, D.W.C.; Zeng, W.; Mei, J.; Zhang, M. Finite element analysis of locking plate and two types of intramedullary nails for treating mid-shaft clavicle fractures. *Injury* **2016**, *47*, 1618–1623. [CrossRef] [PubMed]

35. Meeuwis, M.A.; Pull ter Gunne, A.F.; Verhofstad, M.H.J.; van der Heijden, F.H.W.M. Construct failure after open reduction and plate fixation of displaced midshaft clavicular fractures. *Injury* **2017**, *48*, 715–719. [CrossRef] [PubMed]

36. Switaj, P.J.; Fuchs, D.; Alshouli, M.; Patwardhan, A.G.; Voronov, L.I.; Muriuki, M.; Havey, R.M.; Kadakia, A.R. A biomechanical comparison study of a modern fibular nail and distal fibular locking plate in ao/ota 44c2 ankle fractures. *J. Orthop. Surg. Res.* **2016**, *11*, 100. [CrossRef]

37. Chen, Y.N.; Chang, C.W.; Lin, C.W.; Wang, C.W.; Peng, Y.T.; Chang, C.H.; Li, C.T. Numerical investigation of fracture impaction in proximal humeral fracture fixation with locking plate and intramedullary nail. *Int. Orthop.* **2017**, *41*, 1471–1480. [CrossRef]

38. Zhang, Y.K.; Wei, H.W.; Lin, K.P.; Chen, W.C.; Tsai, C.L.; Lin, K.J. Biomechanical effect of the configuration of screw hole style on locking plate fixation in proximal humerus fracture with a simulated gap: A finite element analysis. *Injury* **2016**, *47*, 1191–1195. [CrossRef]